



HAL
open science

Effect of cysteamine hydrochloride-loaded liposomes on skin depigmenting and penetration

Carla Atallah, Celine Viennet, Sophie Robin, Sami Ibazizen, H el ene Greige-Gerges, Catherine Charcosset

► To cite this version:

Carla Atallah, Celine Viennet, Sophie Robin, Sami Ibazizen, H el ene Greige-Gerges, et al.. Effect of cysteamine hydrochloride-loaded liposomes on skin depigmenting and penetration. *European Journal of Pharmaceutical Sciences*, 2022, 168, pp.106082. 10.1016/j.ejps.2021.106082 . hal-03759788

HAL Id: hal-03759788

<https://hal.science/hal-03759788v1>

Submitted on 24 Aug 2022

HAL is a multi-disciplinary open access archive for the deposit and dissemination of scientific research documents, whether they are published or not. The documents may come from teaching and research institutions in France or abroad, or from public or private research centers.

L'archive ouverte pluridisciplinaire **HAL**, est destin ee au d ep ot et  a la diffusion de documents scientifiques de niveau recherche, publi es ou non,  emanant des  tablissements d'enseignement et de recherche fran ais ou  trangers, des laboratoires publics ou priv es.

1 **Effect of cysteamine hydrochloride-loaded liposomes on skin depigmenting**
2 **and penetration**

3 Carla Atallah^{a,b}, Celine Viennet^c, Sophie Robin^d, Sami Ibazizen^d, H el ene Greige-Gerges^a, and
4 Catherine Charcosset^b

5 *^aBioactive Molecules Research Laboratory, Faculty of Sciences, Lebanese University,*
6 *Lebanon.*

7 *^bLaboratoire d'Automatique, de G enie des Proc ed es et de G enie Pharmaceutiques*
8 *(LAGEPP), Universit e Claude Bernard Lyon 1, France.*

9 *^cUMR 1098 RIGHT INSERM EFS BFC, DImaCell Imaging Ressource Center, University of*
10 *Bourgogne Franche-Comt e, Besan on, 25000, France*

11 *^dBioexigence SAS, Espace Lafayette, Besan on, France*

12

13

14 **Abstract**

15 Skin hyperpigmentation is caused by an excessive production of melanin. Cysteamine, an
16 aminothioliol compound physiologically synthesized in human body cells, is known as
17 depigmenting agent. The aim of this study was to evaluate the depigmenting activity and skin
18 penetration of liposome formulations encapsulating cysteamine hydrochloride. First,
19 cysteamine hydrochloride-loaded liposomes were prepared and characterized for their size,
20 polydispersity index, zeta potential and the encapsulation efficiency of the active molecule. The
21 stability of cysteamine hydrochloride in the prepared liposome formulations in suspension and
22 freeze-dried forms was then assessed. The *in vitro* cytotoxicity of cysteamine and cysteamine-
23 loaded liposome suspensions (either original or freeze-dried) was evaluated in B16 murine
24 melanoma cells. The measurement of melanin and tyrosinase activities was assessed after cells
25 treatment with free and encapsulated cysteamine. The antioxidant activity of the free and
26 encapsulated cysteamine was evaluated by the measurement of ROS formation in treated cells.
27 The *ex vivo* human skin penetration study was also performed using Franz diffusion cell. The
28 stability of cysteamine hydrochloride was improved after encapsulation in liposomal
29 suspension. In addition, for the liposome re-suspended after freeze-drying, a significant increase
30 of vesicle stability was observed. The free and the encapsulated cysteamine in suspension
31 (either original or freeze-dried) did not show any cytotoxic effect, inhibited the melanin
32 synthesis as well as the tyrosinase activity. An antioxidant activity was observed for the free
33 and the encapsulated cysteamine hydrochloride. The encapsulation enhanced the skin
34 penetration of cysteamine hydrochloride. The penetration of this molecule was better for the re-
35 suspended freeze-dried form than the original liposomal suspension where the drug was found
36 retained in the epidermis layer of the skin.

37 **Keywords:** Cysteamine hydrochloride, cystamine, cytotoxicity, liposome, melanin, skin
38 penetration, tyrosinase.

39 **1 Introduction**

40 Many compounds such as hydroquinone, kojic acid, and arbutin are used to treat
41 hyperpigmentation; however, their use was associated with cytotoxic effects (Ephrem et al.,
42 2017; Rendon & Gaviria, 2005; Solano et al., 2006). Cysteamine (cyst), an aminiothiol
43 synthesized by human body cells; and its disulfide form, cystamine, have shown to possess a
44 depigmenting effect on black gold fish (Chavin & Schlesinger, 1966; Frenk et al., 1968).
45 Besides, the application of cysteamine Cream® on the ear of black female guinea pigs
46 demonstrated a high depigmenting effect (Hsu et al., 2013). A randomized, double-blind
47 vehicle-controlled clinical trial was also conducted to evaluate the efficacy and safety of this
48 cream to treat epidermal melasma; the treatment with cysteamine cream® decreased the content
49 of melanin (Farshi et al., 2017; Mansouri et al., 2015). It was reported that the depigmenting
50 action of cyst and cystamine is due to the inhibition of tyrosinase activity which is the enzyme
51 that plays a crucial role in the melanogenesis. Unlike hydroquinone, cyst and cystamine
52 mechanisms of action are a melanogenesis inhibition and not a melanocytotoxicity (Qiu et al.,
53 2000). Qiu et al. reported that 100 μM of cyst inhibit 21% of melanin and 87% of tyrosinase
54 while 50 μM of cystamine inhibit 5% of melanin and 89% of tyrosinase (Qiu et al., 2000).
55 These molecules could also reduce the reactive oxygen species (ROS) generation and enhance
56 the intracellular glutathione (Lee et al., 2017; Okamura et al., 2014; Ribeiro et al., 2013; Shin
57 et al., 2011; Sun et al., 2010). The production of (ROS) was significantly suppressed by low
58 dose of cyst on 1-methyl-4-phenyl-1,2,3,6-tetrahydropyridine-induced dopaminergic
59 neurodegeneration mice (Sun et al., 2010). Cyst also inhibited tert-butyl hydroperoxide-induced
60 ROS production in human corneal endothelial cells (Shin et al., 2011). It reduced ROS
61 production by 33% in phorbol 12-myristate-13-acetate stimulated macrophages (Okamura et
62 al., 2014). In addition, cyst inhibited vascular endothelial growth factor-induced ROS
63 generation in a concentration-dependent manner, with maximum effect at 50 μM (Lee et al.,

64 2017). Moreover, cystamine decreased ROS levels evoked by H₂O₂ or staurosporine in mutant
65 cells (Ribeiro et al., 2013).

66 However, cyst presents an offensive odor and is unstable in solutions where it undergoes
67 oxidation to cystamine (Atallah, Charcosset, et al., 2020). The encapsulation of many skin
68 whitening agents in delivery systems improved their stability (Ephrem et al., 2017). Moreover,
69 it increased their concentration at the targeted site by improving skin permeation, penetration
70 or distribution (Ephrem et al., 2017). Liposomes are nanometric spherical vesicles able to
71 encapsulate hydrophilic, hydrophobic and amphiphilic molecules. They are biodegradable,
72 biocompatible and present a low toxicity (Zylberberg & Matosevic, 2016).

73 Cyst can be used in different forms such as cyst (base form), cyst hydrochloride (cyst HCl),
74 phosphocyst, and cyst bitartrate (**Figure 1**). An increase of the stability of the base form of cyst
75 was previously demonstrated after encapsulation in liposomes suspension (original and from
76 freeze-dried form) compared to free cyst (base form) during storage at 4°C (Atallah, Greige-
77 Gerges, et al., 2020). However, after 60 hours, the remaining cyst in liposome suspension was
78 very low. Therefore, cyst HCl was used in this study because the salt form of this molecule is
79 more stable than its base form (Wiedmann & Naqwi, 2016).

80 The aim of this study was to investigate the effect of cyst HCl-loaded liposomes on
81 melanogenesis and oxidative stress in cultured B16 cells. Skin penetration assays were also
82 conducted on *ex-vivo* human skin. Blank and cyst HCl-loaded liposomes were prepared by the
83 ethanol injection method and characterized for their size, polydispersity index and zeta
84 potential. The encapsulation efficiency of cyst HCl (EE%) in liposomes was also calculated.
85 The amount of residual ethanol in the blank liposomes was determined by NMR technique.
86 Blank and cyst HCl-loaded liposomes were freeze-dried according to the optimized protocol
87 previously described (Gharib et al., 2018). The lyophilized liposomes were then re-suspended
88 with ultra-pure water. The stability of free cysteamine dissolved in water and that of the cyst

89 HCl-loaded liposome suspensions (original or freeze-dried form) was evaluated at 4°C during
90 6 months. The cytotoxicity of free cyst HCl, cystamine and the suspensions of blank- and cyst
91 HCl-loaded liposomes (original or freeze-dried) were evaluated by MTT assay. In addition, the
92 effects of the same formulations on the *in vitro* melanin content and tyrosinase activity were
93 measured. Moreover, the antioxidant activity of the free and the encapsulated cyst HCl was
94 assessed by the measurement of ROS formation induced by the presence of H₂O₂ in B16 cells.
95 Finally, the skin penetration of free- and cyst HCl-loaded liposomes was compared using the
96 Franz diffusion cell.

97 **2 Materials and Methods**

98 **2.1 Materials**

99 Cyst HCl, cystamine dihydrochloride, metformin hydrochloride, (3-(4, 5-dimethylthiazol-2-
100 yl)-2, 5-diphenyltetrazolium bromide), DMSO, L-DOPA and NaOH were purchased from
101 Sigma-Aldrich (Buchs, Switzerland). Phospholipon 90H (90% soybean PC, 4% lysoPC, 2%
102 triglycerides, 2% water, and 0.5% ethanol) was obtained from Lipoid GmbH (Ludwigshafen,
103 Germany). Cholesterol was obtained from the Fisher chemical (Loughborough, UK). HP- β -
104 CD-oral grade (MS=0.85) was purchased from Roquette (Lestrem, France). Sodium dodecyl
105 phosphate and phosphoric acid were obtained from Sigma-Aldrich (China). (trimethylsilyl)-
106 2,2,3,3-tetradecylpropanoic acid sodium salt, 2,7-dichlorodihydrofluorescein diacetate and
107 H₂O₂ were purchased from Sigma-Aldrich (USA). Deuterium oxide (D₂O) was purchased from
108 Acros organics (USA). Dulbecco's Modified Eagle Medium (DMEM), fetal bovine serum
109 (FBS), penicillin, and streptomycin were purchased from Dominique Dutscher (France). All
110 other chemicals were of analytical grade.

111 **2.2 Cyst HCl-loaded liposomes suspensions preparation (original and re-suspended** 112 **after freeze-drying)**

113 Liposomes were prepared by ethanol injection method, as described by Sebaaly et al. (2016).
114 The organic phase was prepared by dissolving phospholipon 90H (saturated lipid) (100 mg)
115 and cholesterol (50 mg) in absolute ethanol (10 mL). Then, the organic phase was injected into
116 the aqueous phase (20 mL) containing 5 mg/mL of cyst HCl, using a syringe pump (Fortuna
117 optima, GmbH-Germany), at a temperature above the transition temperature of the
118 phospholipid (55°C) and under magnetic stirring at 400 rpm. The contact between the organic
119 solution and the aqueous phase leads to a spontaneous liposome formation. The liposomal
120 suspensions were then left for 15 min at 25°C under stirring (400 rpm). The ethanol was
121 removed by rotary evaporation (Heidolph GmbH, Germany) under reduced pressure at 40°C

122 and the obtained liposomal solutions were stored at 4°C. Each preparation was performed in
123 triplicate.

124 The freeze drying of blank- and cyst HCl-loaded liposomes was done as previously reported
125 (Atallah, Greige-Gerges, et al., 2020). In brief, blank liposomes and cyst HCl-loaded liposomes
126 (PH 90H: Chol: cyst molar ratios 1:0.98:10) were freshly prepared; 5 mL were then
127 ultracentrifuged at 170,000g for 1 h at 4 °C. The supernatant was removed, and the pellet was
128 re-dissolved in an aqueous solution of 50 mM HP-β-CD (2 mL). The samples were kept at -20
129 °C overnight then placed into the drying chamber of Cryonext 23,020 freeze-dryer (Trappes,
130 France), pre-cooled to -20°C, then lowered to -40°C with a slow cooling profile of 0.5°C/min.
131 The product was stabilized for 30 min at -38 °C before the vacuum was applied. Primary drying
132 was executed at a pressure of 150 µbar for 3 h at -10°C, then the temperature of the drying
133 chamber was progressively increased to 5 °C for 6 h at 250 µbar, to reach finally 10°C at 350
134 µbar for 9 h. A secondary drying step for 10 h at 20°C and 100 µbar pressure was applied.
135 Finally, the vials were removed from the freeze-dryer, closed with rubber caps, and stored at
136 4°C. The lyophilized liposomes were then re-suspended with ultra-pure water to the original
137 volume (5 mL).

138 **2.3 Cyst HCl-loaded liposomes characterization**

139 The size, polydispersity index and zeta potential were determined using Malvern Zetasizer
140 Nanoseries (Zetasizer Nano ZS; Malvern Instruments Ltd, France). All batches were diluted
141 with ultrapure water. The particle-size distribution data were collected using the DTS (nano)
142 software (version 5.10) provided with the instrument. Zeta potential was calculated using
143 Smoluchowski's equation from the electrophoretic mobility of liposomes. All measurements
144 were carried out at 25°C after 2 min of equilibration and were performed in triplicate. Data
145 were expressed as the mean values ± SD.

146 For the calculation of EE%, liposomal suspensions (5 mL) were ultra-centrifuged (Optima™
147 Ultracentrifuge, Beckman Coulter, USA) at 170,000g for 1 h at 4°C to separate the free cyst
148 HCl (supernatant) from the liposomes loading cyst HCl (pellet). The pellet was re-suspended
149 in water (5 mL). The total liposomal suspension as well as the re-suspended pellet were
150 sonicated and then analyzed by ion pair chromatography method as described below. This
151 allows to determine the total and encapsulated cyst HCl in the liposomal suspensions.
152 The encapsulation efficiency (EE %) of cyst HCl was calculated using the formula:

$$153 \quad EE_{\text{Cyst HCl}} \% = \frac{[\text{Cyst HCl}]_{\text{encapsulated}}}{[\text{Cyst HCl}]_{\text{total}}} \times 100$$

154 Where $[\text{Cyst HCl}]_{\text{encapsulated}}$ and $[\text{Cyst HCl}]_{\text{total}}$ represent the concentration of encapsulated cyst
155 HCl (pellet) and the concentration of the total cyst HCl present in the liposomal suspension,
156 respectively.

157 **2.4 Cyst HCl and cystamine quantification**

158 To quantify cyst HCl and cystamine in the different formulations, an ion-pair chromatography
159 with an isocratic mode consisting of acetonitrile:water containing 0.1% phosphoric acid and
160 sodium dodecyl phosphate (4 mM) (v/v, 45:55) was used. The column was a reverse-phase
161 Kinetex C18 column (4.6 × 100 mm, 2.6 μm). 20 μL were injected in the column maintained at
162 25°C with a flow rate of 1.0 mL/min, and the detection wavelength was 215 nm. Metformin (1
163 μg/mL) was used as an internal standard. Linearity was between 2.5 and 100 μg/mL for cyst
164 HCl and between 5 and 100 μg/mL for cystamine. This method was previously used for the
165 quantification of cyst in its base form; the same chromatographic results were obtained as for
166 cyst HCl (retention time, limits of detection and quantification).

167 **2.5 Ethanol quantification in the blank liposomal suspension**

168 The quantity of ethanol present in the blank liposomal suspension was also determined by NMR
169 technique according to Zuriarrain et al. (Zuriarrain et al., 2015). Blank liposomal suspensions

170 were centrifuged for 10 min at 11200g. The residual ethanol is supposed to be present in the
171 upper phase. The internal standard used was (trimethylsilyl)-2,2,3,3-tetra-deutero-propionic
172 acid sodium salt (TSP) $(\text{CH}_3)_3\text{SiCD}_2\text{CD}_2\text{CO}_2\text{Na}$. 10 mg of TSP was dissolved in 400 μL D_2O
173 and 300 μL of the supernatant of the liposomal suspension. The number of moles of ethanol is
174 calculated from the NMR spectrum using the following equation:

$$175 \quad n_{\text{EtOH}} = \frac{H_{\text{IS}}}{H_{\text{CH}_2}} \times n_{\text{IS}} \times \frac{I_{\text{CH}_2}}{I_{\text{IS}}}$$

176 Where H_{IS} and H_{CH_2} are the numbers of hydrogen atoms present in the internal standard
177 structure (equals to 9) and in CH_2 group of ethanol (equals to 2), n_{IS} is the number of moles of
178 the internal standard (equals to 5.78×10^{-5} mole) and I_{CH_2} and I_{IS} are the integration of the CH_2
179 group of ethanol and the internal standard peaks.

180 To simplify, we replaced H_{IS} , H_{CH_2} and n_{IS} by their values to obtain the following equation:

$$181 \quad n_{\text{EtOH (mole)}} = 0.00026 \times \frac{I_{\text{CH}_2}}{I_{\text{IS}}}$$

182 **2.6 Stability of free cyst HCl in solution, suspended cyst HCl-loaded liposomes**

183 **(original and freeze-dried)**

184 The stability of cyst HCl-loaded liposome was compared to that of free cyst HCl. The liposomal
185 suspension (5 mL) was centrifuged, the supernatant was eliminated, and the pellet was re-
186 suspended in water. The concentration of the encapsulated cyst HCl was determined after the
187 destruction of liposomes by sonication. A solution of cyst HCl with the same concentration of
188 the encapsulated cyst HCl was also prepared in water and stored at 4°C. After 6 months of
189 storage at 4 °C, the concentration of the remaining cyst HCl in free cyst HCl solution and the
190 suspensions of liposomes loading cyst HCl was determined. Also, after three months of storage
191 at 4 °C, freeze-dried liposomes were re-suspended in 5 mL water and the remaining cyst HCl
192 concentration was measured using ion-pair chromatography.

193 **2.7 Cell culture**

194 B16 murine melanoma cells (Elabscience, CliniSciences, Nanterre, France) were grown in
195 Dulbecco's Modified Eagle Medium (DMEM) supplemented with 10% heat-inactivated fetal
196 bovine serum (FBS), 100 U/mL penicillin, and 100 µg/mL streptomycin. Cells were maintained
197 in an incubator at 37 °C in a humidified 5% CO₂ atmosphere and passaged weekly using trypsin
198 0.05%/EDTA 0.02% in PBS to maintain the optimum conditions for exponential growth.

199 **2.8 Preparation of the formulations**

200 Different concentrations of cyst HCl and cystamine (50; 60; 100 and 500 µM) were prepared
201 in culture medium. Blank liposomes (original and re-suspended after freeze-drying) were
202 prepared between 0.1 to 5.7% v/v in culture medium to evaluate their cytotoxic effect. The
203 suspensions containing total cyst HCl-loaded liposome (encapsulated and non-encapsulated)
204 were centrifuged and the pellet was re-suspended to obtain the encapsulated cyst HCl-loaded
205 liposome. The total (present in the whole suspension) and the encapsulated cyst HCl-loaded
206 liposome were diluted in culture medium to obtain 0.1 and 2.8 v/v%, respectively. The freeze
207 dried cyst HCl-loaded liposomes were re-suspended in water and then diluted in culture
208 medium to obtain 5.7 v/v%. These dilutions were made to obtain the same concentration of cyst
209 HCl (60 µM) in all formulations. Kojic acid (700 µM) was prepared in water and used as
210 positive control.

211 **2.9 Cytotoxicity analysis**

212 B16 melanoma cell viability was determined by the (3-(4, 5-dimethylthiazol-2-yl)-2, 5-
213 diphenyltetrazolium bromide) MTT assay. Cells were seeded in 96-well microtiter plates at a
214 density of 6×10^3 cells/well. After 24 h of incubation at 37°C in 5% CO₂, cells were treated with
215 100 µL of each formulation described in section 2.8. After 24 and 48 h of incubation with the
216 different formulations, the medium was removed, cells were washed twice and 100 µL of MTT
217 solution (0.5 mg/mL in medium) were added to each well. Cells were incubated for 4 h at 37°C

218 and the produced formazan salts were then dissolved in DMSO. Absorbance was measured at
219 571 nm by spectroscopy on a microplate reader (Thermo Scientific, Multiskan FC).

220 **2.10 Melanin measurement**

221 B16 cells were seeded at a density of 10×10^4 cells/well in 6-well plates. Plates were incubated
222 for 24 h at 37°C in 5% CO₂ before being treated with cyst HCl (60 μM), cystamine (60 μM),
223 kojic acid (700 μM), blank liposomes (original suspension and re-suspended freeze-dried form),
224 total cyst HCl-loaded liposome suspension, encapsulated cyst HCl-loaded liposome suspension
225 and suspended freeze-dried cyst HCl-loaded liposome. After 24 and 48 h, cells were collected
226 by scraping into ice-cold PBS and pelleted. Intracellular melanin was extracted by solubilizing
227 cell pellets in 1N NaOH containing 10% DMSO for 2 h at 80°C. The melanin content of cell
228 lysate supernatants was measured spectrophotometrically at an absorbance of 405 nm against a
229 standard curve of synthetic melanin. Intracellular melanin content was adjusted by the amount
230 of protein.

231 **2.11 Tyrosinase activity assay**

232 Intracellular tyrosinase activity was determined by measuring the rate of oxidation of L-DOPA
233 to DOPACHrome. B16 cells were seeded at a density of 10×10^4 cells/well in 6-well plates. After
234 24 h, 2 mL of cyst HCl (60 μM), cystamine (60 μM), kojic acid (700 μM), blank liposomes
235 (original suspension and re-suspended after freeze-drying), whole suspension of cyst HCl-
236 loaded liposome, suspended cyst HCl-loaded liposome (encapsulated) and suspended freeze-
237 dried cyst HCl-loaded liposome were added to cells. 48 and 72h post-treatment, cells were
238 harvested by scraping into ice-cold PBS and lysed at room temperature for 15 min with 0.5%
239 Triton X-100 in PBS. Lysed cell supernatants (100 μL) were mixed with 100 μL of freshly
240 prepared L-DOPA solution (0.1% in PBS). Following incubation at 37°C for 1 h, absorbance
241 was measured at 450 nm and compared with a standard curve using mushroom tyrosinase.

242 Tyrosinase activity was normalized to the amount of protein (determined using the Bradford
243 assay).

244 **2.12 Reactive oxygen species content**

245 Intracellular ROS production was detected using the oxidation-sensitive fluorescence dye 2,7-
246 dichlorodihydrofluorescein diacetate (DCFH-DA). Cells were seeded at a density of 6×10^3
247 cells/well in 96-well plates. After 24 h, they were firstly treated 2 times over a period of 72 h
248 with 100 μL of tested substances, and secondly treated with H_2O_2 (100 μM in culture medium)
249 for 6 h. Then DCFH-DA solution (1 μM in culture medium) was added to cells for 30 min at
250 37°C . Immediately after PBS washing, fluorescence was quantified using a
251 spectrofluorophotometer (BioTek, Synergy H1) with 495 nm excitation and 527 nm emission
252 filters. ROS were observed under an inverted fluorescence microscope (Olympus, DP50).

253 **2.13 *Ex vivo* skin penetration study with Franz cell**

254 *Ex vivo* percutaneous permeation of cyst HCl was performed on thawed skin from a female
255 caucasian donor. Skin was defatted using a scalpel and then dermatomed with a dermatome
256 (Zimmer Biomet Electric® Dermatome). Skin discs were realized using a circled cutter and the
257 thickness range was between 400 and 600 microns. Skin discs were mounted on a Franz cells
258 system (PermeGear). Franz cells were previously filled with receptor fluid (RF) consisting of
259 PBS-EDTA 0.1% at pH 7.4. Skin discs were equilibrated during 1 h before measurement of
260 TEWL (Trans Epidermal Water Loss) using a tewameter TM300 (MDD 4, Courage &
261 Khazaka). The tested formulations were cyst HCl solution, total and encapsulated cyst HCl-
262 loaded liposomes and resuspended freeze-dried cyst HCl-loaded liposomes. 1 mL of each
263 formulation diluted to obtain $1200\mu\text{M}$ of cyst HCl as a final concentration has been deposited
264 on the skin. RF was sampled at different time points 0, 1, 4, 18 and 24h. At 24 h, formulations
265 were removed and skin discs were washed with RF (1 mL). Skin compartments were separated
266 using forceps in order to obtain epidermis and dermis. Samples (Washing, Epidermis and

267 Dermis) were weighed and then the active ingredient was extracted in methanol:water
268 extraction solvent (50:50, v/v) after stirring during 24 h. Finally, extracts were quantified by
269 ion pair chromatography.

270 **2.14 Statistical analysis**

271 The differences between the treated and the control cells were calculated using ANOVA
272 (GraphPad Prism 9; GraphPad Software, San Diego, CA) with $p < 0.05$ defining statistical
273 significance.

274 **3 Results and discussion**

275 **3.1 Characterization of cyst HCl-loaded liposomes**

276 The sizes of the blank and cyst HCl-loaded liposomes were similar with 211 ± 8 nm and $217 \pm$
277 22 nm for blank and loaded liposomes, respectively. The polydispersity index was 0.2 ± 0.1 for
278 the blank and cyst HCl-loaded liposomes indicating that the liposomal population was
279 homogeneous. The zeta potential of the blank liposomes (-17.95 ± 4.0 mV) was increased after
280 the addition of cyst HCl (-2.37 ± 0.7 mV). This result indicates the presence of an interaction
281 between cyst HCl and the liposomal suspension. The EE% of the studied formulation was 3.74
282 ± 0.46 % which is lower than the EE% of cyst-loaded liposome ($21 \pm 5.0\%$) found in our
283 previous work using the base form of cyst (Atallah, Greige-Gerges, et al., 2020). Cyst (base
284 form) and cyst HCl differ by their aqueous solubility, pH of their aqueous solution, and their
285 stability. The base form may interact with negatively charged phosphate of phospholipids
286 leading to a greater encapsulation when compared with cyst HCl form.

287 The remaining percentage of ethanol in the liposomal suspension depended on the time of
288 evaporation and the remaining volume of liposomal suspension. In fact, the percentage of the
289 ethanol in the liposomal suspension increased with the increase of the final volume of liposomal
290 suspension. The percentage of ethanol in all the studied conditions was less than 2.6% (**Table**
291 **S1**).

292 **3.2 Stability of cyst HCl-loaded liposomes**

293 The stability of cyst HCl-loaded liposomes and free cyst HCl prepared in water was assessed
294 after storage at 4°C. The total degradation of free cyst HCl was obtained after 16 days, whereas
295 a remaining cyst HCl percentage of 9.5% was obtained in the cyst HCl-loaded liposomes in
296 suspension form after 6 months of storage at 4°C. The total concentration of cyst HCl in the
297 resuspended freeze dried liposomes was determined after 3 months of storage at 4°C showing
298 that the concentration of cyst HCl determined at time 0 was stable after 3 months of storage

299 **(Figure 2)**. The stability of cysteamine in its hydrochloride form was much better than in its
300 base form. For the same concentration of the free drug (200 µg/mL), cysteamine in its base
301 form was totally converted to cystamine after 15h of storage at 4°C (Atallah, Greige-Gerges, et
302 al., 2020) while cyst HCl was totally converted after 16 days of storage at 4°C. The
303 encapsulation of cyst HCl increased its stability in suspension form (total degradation after 6
304 months of storage) and for a longer time when the formulation was freeze-dried (no degradation
305 after 3 months of storage). The base form of cyst (200 µg/mL) was totally oxidized after 60 h
306 in the liposomal suspension and 4 months in the freeze-dried form (Atallah, Greige-Gerges, et
307 al., 2020).

308 **3.3 Cytotoxicity of blank liposomes (original suspension and suspended freeze-dried** 309 **form)**

310 The cytotoxicity of the blank liposomes in suspension and the suspended freeze-dried form was
311 evaluated by MTT assay on B16 murine melanoma cells after 24 and 48 h of incubation.
312 Following the ISO 10993-5 guideline, percentages of cell viability above 80% are considered
313 as non-cytotoxic. Blank liposomes in suspension form did not show any cytotoxic effect at the
314 various volume concentrations (0.1; 1; 2; 2.8 and 5% v/v) (**Table S2**). 5% of H₂O/ethanol
315 solution decreased the cell viability to 83 ± 0.1%. Suspended freeze-dried blank liposomes
316 showed a higher cytotoxicity than the liposomal suspension after 24 h of incubation. For 5%
317 (v/v), the cytotoxicity of blank liposomal suspension was 90 ± 0.1% while it was 75 ± 0.1% for
318 the suspended freeze-dried form (**Table S2**). The cytotoxicity of the liposomes decreased after
319 48 h. The cytotoxicity observed is probably due to the presence of the HP-β-CD (used as a
320 cryoprotectant) in the freeze-dried vesicles (Hammoud et al., 2019).

321 **3.4 Cytotoxicity of free cyst HCl and cystamine**

322 The cytotoxicity of free cyst HCl and cystamine was for the first time evaluated on B16
323 melanoma cell line. Free cyst HCl and cystamine did not show any cytotoxicity between 50 and

324 100 μM (cell viability > 92%). However, cystamine showed a higher cytotoxicity than cyst HCl
325 at 500 μM ; cell viability was decreased to $59 \pm 0.1\%$ and $26 \pm 0.1\%$ after 24h of 500 μM cyst
326 HCl and cystamine treatments, respectively (**Figure 3A**). Similarly, Qiu et al. showed that
327 cystamine (50 to 100 μM) did not present any cytotoxic effect on MM418c5, MM96L and HeLa
328 cells after 6 days of treatment (Qiu et al., 2000). According to these results, cyst HCl at a
329 concentration of 60 μM was chosen for the next analysis.

330 **3.5 Cytotoxicity of cyst HCl-loaded liposomes**

331 The cytotoxicity of the total and encapsulated cyst HCl loaded liposomes was also evaluated
332 on B16 melanoma cells. Cell viability of the total and encapsulated cyst HCl-loaded liposomes
333 was $92 \pm 0.1\%$ and $95 \pm 0.1\%$, respectively, after 24 h of incubation. However, the suspended
334 freeze-dried form was more cytotoxic ($74 \pm 0.1\%$) than the liposomal suspension (**Figure 3B**).

335 **3.6 Inhibition of melanin synthesis**

336 To study the effect of cyst HCl loaded liposomes on melanogenesis, we examined the level of
337 melanin produced in B16 cells after 2 treatments during 72 h of incubation with free cyst HCl
338 and cystamine (culture media as control), whole liposome suspension encapsulating cyst HCl
339 and cyst HCl-loaded liposome (original liposome suspension as control), and resuspended
340 freeze-dried cyst HCl-loaded liposome (resuspended freeze-dried liposome as control). Kojic
341 acid was used as a positive control.

342 For the same concentration of cyst HCl and cystamine (60 μM), cystamine was able to reduce
343 the melanin content in the cells ($33.0 \pm 13.0\%$) more than cyst HCl ($26.0 \pm 8.6\%$). Kojic acid
344 used as a reference presented a melanin inhibition of $36.0 \pm 9.1\%$. Suspended freeze-dried blank
345 liposome did not show any inhibition of melanin (data not shown). The inhibition of melanin
346 was lower for the encapsulated ($22.0 \pm 0.9\%$) form compared to the free form ($26.0 \pm 8.6\%$).
347 The suspended freeze-dried cyst HCl-loaded liposome ($23.5 \pm 6.3\%$) showed a better inhibition
348 of melanin than the original suspension (**Figure 4**).

349 **3.7 Inhibition of tyrosinase activity**

350 The tyrosinase enzyme plays a crucial role in melanogenesis. Kojic acid (used as positive
351 control) showed a strong inhibition of the enzyme activity ($36.2 \pm 5.8\%$). Cystamine ($28.2 \pm$
352 12.2%) and cyst HCl ($26.8 \pm 5.5\%$) inhibited the tyrosinase activity. Therefore, melanogenesis
353 inhibition by cyst HCl and cystamine in B16 cells occurs via direct inhibition of tyrosinase
354 activity, as previously described by Qiu et al. The effect of the cyst HCl encapsulated in
355 liposomes on the inhibition of the tyrosinase activity was investigated. The encapsulation of
356 cyst HCl decreased its inhibition of tyrosinase activity effect ($26.8 \pm 5.5\%$ was inhibited in
357 presence of free cyst HCl while $19.6 \pm 4.4\%$ and $18.3 \pm 2.9\%$ was inhibited for the encapsulated
358 cyst HCl loaded liposome and resuspended freeze-dried cyst HCl-loaded, respectively) (**Figure**
359 **4**).

360 To the best of our knowledge, one study investigated the depigmenting effect of cyst *in vitro*
361 using pigmented melanoma MM418c5 cells. It showed that $100 \mu\text{M}$ of cyst inhibit 21.0% of
362 melanin and 87.0% of tyrosinase while $50 \mu\text{M}$ of cystamine inhibit 5.0% of melanin and 89.0%
363 of tyrosinase (Qiu et al., 2000).

364 **Figure 5** shows the microscopic observation of the cells after 2 treatments during 72 h of
365 incubation with free, total and encapsulated cyst HCl-loaded liposome in suspension and
366 resuspended freeze-dried forms. It also shows the solubilized cell pellets of the different treated
367 cells. A whitening effect was observed for all the formulations in comparison with the control.

368 **3.8 Reactive oxygen species content**

369 Intracellular oxidative stress was measured by the DCFH-DA assay. The cleavage of two
370 acetate groups of DCFH-DA by esterase will lead to the formation of DCFH that can be
371 oxidized to a highly fluorescent compound DCF by intracellular ROS. Therefore, the
372 fluorescence intensity of DCF can directly reflect the level of ROS in the cell (Rhee et al.,

2010). Hydrogen peroxide (H_2O_2) is a well-known inducer of oxidative stress. To estimate the effect of cyst HCl and its encapsulation on the intracellular production of ROS in cultured B16 cells, cells were pretreated 2 times over a period of 72 h with 60 μM of cyst HCl and cystamine; total and encapsulated cyst HCl-loaded liposome in suspension and resuspended freeze-dried forms, and then treated for 6 h with H_2O_2 . The inhibited percentage of ROS formation was 43.4 \pm 10.3% and 38.6 \pm 9.8% in the presence of free cyst HCl and cystamine, respectively. This percentage was slightly decreased after the encapsulation of cyst HCl where it was 35.4 \pm 10.1% and 33.6 \pm 11.6% for the encapsulated cyst HCl in suspension and resuspended freeze dried forms (**Figure 6**). After, the addition of 60 μM cyst or cystamine to the B16 cells, a decrease in ROS levels by a factor of 1.8 and 1.6, respectively, in comparison with the control was observed. The addition of the encapsulated cyst HCl in suspension and resuspended freeze dried forms also decreased the relative fluorescence by 1.4 and 1.5 times in comparison with the control. **Figure 7** shows fluorescence microscopy images of B16 cells. A decrease of the DCFH-DA fluorescence in all cultures treated with the formulations containing cyst HCl was observed in comparison to the control.

3.9 Skin penetration study

The cumulative amounts of cyst HCl penetrating the skin and found in the receptor fluid from each of the liposomal formulation and controls over 24 h are shown in **Figure 8**. The encapsulation of cyst HCl in liposomes increased its penetration through the human skin. The quantity of cyst HCl found in the fluid receptor after 24 h of deposition was increased by 2.9-; 3.5- and 3.5-fold for the total, encapsulated and lyophilized cyst HCl loaded liposomes, respectively in comparison to the free drug in solution (**Figure 8**). Cystamine did not penetrate the skin since it was not found in the receptor fluid nor in the epidermis layer.

Figure 9 shows the retention of cyst HCl in the epidermis when the drug was free or encapsulated in liposomes in suspension or in resuspended freeze-dried forms. The highest

398 quantity of retained cyst HCl in the epidermis was found for the cyst HCl-loaded liposome in
399 the resuspended freeze-dried form ($150 \mu\text{g}/\text{cm}^2$). The presence of HP- β -CD could be the reason
400 behind the increase of cyst penetration in the resuspended freeze-dried form. The cyclodextrin
401 is known to be a penetration enhancer of the drug through the membranes (Loftsson &
402 Sigurdardóttir, 1996; Yan et al., 2014). α -Cyclodextrin demonstrated its ability to promote the
403 trans corneal diffusion of cyst (Pescina et al., 2016). A slight decrease of the retention of the
404 molecule in the epidermis was observed for cyst HCl encapsulated in liposome ($120.0 \mu\text{g}/\text{cm}^2$)
405 in comparison with the free drug ($140.0 \mu\text{g}/\text{cm}^2$) while a higher decrease was obtained for the
406 total cyst HCl loaded liposome ($85.0 \mu\text{g}/\text{cm}^2$). No trace of cystamine was found in the
407 epidermis.

408 **4 Discussion**

409 Liposomes represent the most studied system for drug delivery through the skin. These delivery
410 systems are used to enhance stability, skin penetration, depigmenting effect and antioxidant
411 activity of several compounds. For example, vitamin A demonstrated better stability when
412 loaded into liposomes compared to the free form during exposure to UV radiation (Arsić &
413 Vuleta, 1999). The encapsulation of curcumin in liposomes provided substantially more
414 protection than the encapsulation in CDs (Matloob et al., 2014). Amphotericin B liposome
415 formulations showed a higher stability (shelf life of 1 year) compared to the free drug (4 and
416 14 days) (Manosroi et al., 2004). The chemical stability of fasudil, an anti-vasospastic agent,
417 was also enhanced after its encapsulation (Ishida et al., 2002). In this article, the encapsulation
418 of cyst HCl in liposomes enhanced its stability; the total degradation of cyst HCl was obtained
419 after 16 days in aqueous medium, and lasted for 6 months for the liposomal suspension.
420 Moreover, cyst HCl loaded liposomes were stable during freeze-drying, and stability was
421 maintained after 3 months of storage.

422 In addition, the cream containing liposome-encapsulated 4-n-butylresorcinol and resveratrol
423 was shown to be effective and safe for the treatment of melasma. (Kwon et al., 2020). Aloe
424 Vera loaded into liposomes was proposed for melasma treatment and as an effective skin care
425 formulation especially for anti-aging and skin regeneration (Ghafarzadeh & Eatemadi, 2017).
426 In this study, the encapsulation of cyst HCl in liposomes showed a decrease of the depigmenting
427 effect that could be due to the entrapment of the drug in the liposomes aqueous compartment.
428 Hydroxytyrosol liposomes presented better DPPH radical scavenging activity than free
429 hydroxytyrosol, which could be due to the fact that hydroxytyrosol was encapsulated inside the
430 liposomes with a high encapsulation rate (Yuan et al., 2017). Stronger free radical scavenging
431 effect was obtained in *Orthosiphon stamineus* liposomes than in nonformulated extract (Yücel
432 & Şeker Karatoprak, 2017). No variation of the antioxidant activity was observed for the
433 hydrophilic *Crithmum maritimum* after its encapsulation in liposomes (Alemán et al., 2019).
434 Also, our results are in accordance with Aleman et al. where the antioxidant activity was slightly
435 decreased after encapsulation in liposomes.

436 Liposomes also showed an increase of skin penetration of entrapped and non-entrapped
437 hydrophilic substances into human skin. The penetration study of the liposomal formulation
438 containing encapsulated and non-encapsulated carboxyfluorescein exhibited maximum
439 deposition of this compound in the stratum corneum, whereas the liposomes containing just the
440 encapsulated carboxyfluorescein inside the liposomes showed a higher penetration into deeper
441 skin layers, such as the viable epidermis, and through the skin to the receiver compartment of
442 Franz diffusion cell (Verma et al., 2003). Another study showed that maximum idebenone
443 penetration in dermis was achieved by liposomes compared to leciplex and invasomes (Shah et
444 al., 2015). The skin penetration of itraconazole (ITZ) was studied using an aqueous solution of
445 ITZ, CD/ITZ inclusion complex, ITZ loaded liposomes and the CD/ITZ inclusion complex
446 loaded into liposomes. The complex improved slightly the drug penetration while ITZ-HP- β -

447 CD-loaded liposomes exhibited significant increase in ITZ skin deposition compared to
448 liposomes containing ITZ alone (Alomrani et al., 2014). Our results are in accordance with the
449 literature as an increase of the skin penetration was observed with cyst HCl encapsulation
450 especially the freeze dried form containing HP- β -CD.

451 In this study, phospholipon 90H (PH90H) and cholesterol were chosen to prepare liposomes
452 encapsulating cyst HCl. Previous studies used PH90H liposomes to enhance the skin
453 penetration of drugs of various pharmacological classes, like methotrexate, idoxuridine and
454 acyclovir. It was shown that their dermal penetration was improved (Ita et al., 2010). Tarnowska
455 et al. also used PH90H liposomes to study the skin absorption of Mg^{2+} and Ca^{2+} from thermal
456 spring water, and showed that the suspension improved the skin absorption of Ca^{2+} (Tarnowska
457 et al., 2020). Beside, a mixture of PH90H and cholesterol was used for preparation of liposomes
458 encapsulating terbinafine HCl by the ethanol injection method. The cutaneous application of
459 this formulation prolonged the antifungal activity (Beeravelli et al., 2014). Similarly, a
460 liposomal formulation based on PH90H and cholesterol encapsulating nadifloxacin showed a
461 better penetration in deeper layers of skin, when compared with the free drug (Shiny et al.,
462 2016). In addition, saturated PH90H are in a gel like state on the skin, due to their melting
463 temperature T_m around $50^\circ C$ (Dörfler & Brezesinski, 1983). A study successfully confirmed
464 that hydrogenated phospholipids penetrate into the stratum corneum, a high amount of the
465 lipid was found in the upper skin layers and a gradual decrease was noticed in the deeper layers
466 showing an accumulation of saturated phosphatidylcholine in upper epidermal layers
467 (Gutekunst et al., 2018).

468 Liposomes can be applied on the skin under different forms such as gel or cream. Topical gels
469 are commonly prescribed for skin diseases. The use of topical gels is convenient and could
470 provide a prolonged skin retention of the drug, which is beneficial for the treatment of skin
471 disease. Several studies used the liposomal gel for skin applications. For example, Wang et al.

472 used liposomal gel dual-loaded with all-trans retinoic acid and betamethasone for enhanced
473 therapeutic efficiency of psoriasis (Wang et al., 2020). The dermal delivery of nadifloxacin was
474 enhanced using liposomal gel (Shiny et al., 2016). In addition, liposomal gels were developed
475 for the topical delivery of anthralin (Fathalla et al., 2020).

476 **5 Conclusion**

477 The encapsulation of cyst HCl increased the stability of the molecule especially when the
478 formulation was freeze-dried. The formulation was not cytotoxic with the chosen
479 concentrations. Cyst HCl and cystamine showed an inhibition of melanin and tyrosinase activity
480 but cystamine was not able to penetrate the skin layers. The encapsulation of cyst HCl decreased
481 its inhibition of melanin and tyrosinase activity but increased its penetration in the skin and its
482 retention in the epidermis. The encapsulation didn't affect the antioxidant activity observed for
483 the free cyst HCl. These findings are important for further application of cyst HCl liposomal
484 formulations as a depigmenting agent. In this study, the results of depigmenting and anti-
485 oxidant activities are based on vitro assays, precisely 2D cultures of B16. The *B16 cell* line is a
486 widely used *model* for skin whitening and pigmentation studies. But potentially 3D models
487 where cells are embedded in complex environments offer a better model of the *in vivo* cell
488 environment than traditional 2D culture.

489 **Acknowledgements**

490 Authors thank the Research Funding Program at the Lebanese University and the “Agence
491 Universitaire de la Francophonie, projet PCSI” for supporting the project (2018-2020). Authors
492 also thank the Lyon 1 University NMR facility for setting up the NMR experiments.

493 **Declaration of Competing Interest**

494 The authors declare that they have no known competing financial interests or personal
495 relationships that could have appeared to influence the work reported in this paper.

496 **6 References**

497

498 Alemán, A., Marín, D., Taladrid, D., Montero, P., & Carmen Gómez-Guillén, M. (2019).

499 Encapsulation of antioxidant sea fennel (*Crithmum maritimum*) aqueous and ethanolic
500 extracts in freeze-dried soy phosphatidylcholine liposomes. *Food Research*
501 *International (Ottawa, Ont.)*, 119, 665–674.

502 <https://doi.org/10.1016/j.foodres.2018.10.044>

503 Alomrani, A. H., Shazly, G. A., Amara, A. A., & Badran, M. M. (2014). Itraconazole-

504 hydroxypropyl- β -cyclodextrin loaded deformable liposomes: In vitro skin penetration
505 studies and antifungal efficacy using *Candida albicans* as model. *Colloids and*
506 *Surfaces. B, Biointerfaces*, 121, 74–81. <https://doi.org/10.1016/j.colsurfb.2014.05.030>

507 Arsić, I., & Vuleta, G. (1999). Influence of liposomes on the stability of vitamin a

508 incorporated in polyacrylate hydrogel. *International Journal of Cosmetic Science*,
509 21(4), 219–225. <https://doi.org/10.1046/j.1467-2494.1999.181682.x>

510 Atallah, C., Charcosset, C., & Greige-Gerges, H. (2020). Challenges for cysteamine

511 stabilization, quantification, and biological effects improvement. *Journal of*
512 *Pharmaceutical Analysis*, 10(6), 499–516. <https://doi.org/10.1016/j.jpha.2020.03.007>

513 Atallah, C., Greige-Gerges, H., & Charcosset, C. (2020). Development of cysteamine loaded

514 liposomes in liquid and dried forms for improvement of cysteamine stability.
515 *International Journal of Pharmaceutics*, 119721.

516 <https://doi.org/10.1016/j.ijpharm.2020.119721>

517 Beeravelli, S., J. N., R. V., & K. V., R. M. (2014). Formulation, Characterization and ex vivo

518 Studies of Terbinafine HCl Liposomes for Cutaneous Delivery. *Current Drug*
519 *Delivery*, 11(4), 521–530.

- 520 Chavin, W., & Schlesinger, W. (1966). Some potent melanin depigmentary agents in the
521 black goldfish. *Die Naturwissenschaften*, 53(16), 413–414.
- 522 Dörfler, H.-D., & Brezesinski, G. (1983). Phasenumwandlungerscheinungen in
523 Lecithin/Wasser-Systemen. *Colloid and Polymer Science*, 261(3), 286–292.
524 <https://doi.org/10.1007/BF01469677>
- 525 Ephrem, E., Elaissari, H., & Greige-Gerges, H. (2017). Improvement of skin whitening agents
526 efficiency through encapsulation: Current state of knowledge. *International Journal of*
527 *Pharmaceutics*, 526(1–2), 50–68. <https://doi.org/10.1016/j.ijpharm.2017.04.020>
- 528 Farshi, S., Mansouri, P., & Kasraee, B. (2017). Efficacy of cysteamine cream in the treatment
529 of epidermal melasma, evaluating by Dermacatch as a new measurement method: A
530 randomized double blind placebo controlled study. *Journal of Dermatological*
531 *Treatment*, 1–8. <https://doi.org/10.1080/09546634.2017.1351608>
- 532 Fathalla, D., Youssef, E. M. K., & Soliman, G. M. (2020). Liposomal and Ethosomal Gels for
533 the Topical Delivery of Anthralin: Preparation, Comparative Evaluation and Clinical
534 Assessment in Psoriatic Patients. *Pharmaceutics*, 12(5), 446.
535 <https://doi.org/10.3390/pharmaceutics12050446>
- 536 Frenk, E., Pathak, M. A., Szabó, G., & Fitzpatrick, T. B. (1968). Selective action of
537 mercaptoethylamines on melanocytes in mammalian skin: Experimental
538 depigmentation. *Archives of Dermatology*, 97(4), 465–477.
- 539 Ghafarzadeh, M., & Eatemadi, A. (2017). Clinical efficacy of liposome-encapsulated Aloe
540 vera on melasma treatment during pregnancy. *Journal of Cosmetic and Laser*
541 *Therapy: Official Publication of the European Society for Laser Dermatology*, 19(3),
542 181–187. <https://doi.org/10.1080/14764172.2017.1279329>
- 543 Gharib, R., Greige-Gerges, H., Fourmentin, S., & Charcosset, C. (2018). Hydroxypropyl- β -
544 cyclodextrin as a membrane protectant during freeze-drying of hydrogenated and non-

545 hydrogenated liposomes and molecule-in-cyclodextrin-in- liposomes: Application to
546 trans-anethole. *Food Chemistry*, 267, 67–74.
547 <https://doi.org/10.1016/j.foodchem.2017.10.144>

548 Gutekunst, D., Hoogevest, P., & Heidecke, C. (2018). *The effect of saturated phospholipids*
549 *on human skin assessed with shotgun lipidomic analysis.*

550 Hammoud, Z., Khreich, N., Auezova, L., Fourmentin, S., Elaissari, A., & Greige-Gerges, H.
551 (2019). Cyclodextrin-membrane interaction in drug delivery and membrane structure
552 maintenance. *International Journal of Pharmaceutics*, 564, 59–76.
553 <https://doi.org/10.1016/j.ijpharm.2019.03.063>

554 Hsu, C., Mahdi, H. A., Pourahmadi, M., & Ahmadi, S. (2013). Cysteamine cream as a new
555 skin depigmenting product. *Journal of the American Academy of Dermatology*, 68(4).
556 <https://doi.org/10.1016/j.jaad.2012.12.781>

557 Ishida, T., Takanashi, Y., Doi, H., Yamamoto, I., & Kiwada, H. (2002). Encapsulation of an
558 antivasospastic drug, fasudil, into liposomes, and in vitro stability of the fasudil-
559 loaded liposomes. *International Journal of Pharmaceutics*, 232(1–2), 59–67.
560 [https://doi.org/10.1016/s0378-5173\(01\)00896-1](https://doi.org/10.1016/s0378-5173(01)00896-1)

561 Ita, K. B., Du Preez, J., du Plessis, J., Lane, M. E., & Hadgraft, J. (2010). Dermal delivery of
562 selected hydrophilic drugs from elastic liposomes: Effect of phospholipid formulation
563 and surfactants. *Journal of Pharmacy and Pharmacology*, 59(9), 1215–1222.
564 <https://doi.org/10.1211/jpp.59.9.0005>

565 Kwon, S.-H., Yang, J. H., Shin, J.-W., Park, K.-C., Huh, C.-H., & Na, J.-I. (2020). Efficacy of
566 liposome-encapsulated 4-n-butylresorcinol and resveratrol cream in the treatment of
567 melasma. *Journal of Cosmetic Dermatology*, 19(4), 891–895.
568 <https://doi.org/10.1111/jocd.13080>

569 Lee, Y.-J., Jung, S.-H., Hwang, J., Jeon, S., Han, E.-T., Park, W. S., Hong, S.-H., Kim, Y.-M.,
570 & Ha, K.-S. (2017). Cysteamine prevents vascular leakage through inhibiting
571 transglutaminase in diabetic retina. *Journal of Endocrinology*, 235(1), 39–48.
572 <https://doi.org/10.1530/JOE-17-0109>

573 Loftsson, T., & Sigurdardóttir, A. M. (1996). Cyclodextrins as Skin Penetration Enhancers. In
574 J. Szejtli & L. Szenté (Eds.), *Proceedings of the Eighth International Symposium on*
575 *Cyclodextrins* (pp. 403–406). Springer Netherlands. [https://doi.org/10.1007/978-94-](https://doi.org/10.1007/978-94-011-5448-2_90)
576 [011-5448-2_90](https://doi.org/10.1007/978-94-011-5448-2_90)

577 Manosroi, A., Kongkaneramt, L., & Manosroi, J. (2004). Stability and transdermal
578 absorption of topical amphotericin B liposome formulations. *International Journal of*
579 *Pharmaceutics*, 270(1), 279–286. <https://doi.org/10.1016/j.ijpharm.2003.10.031>

580 Mansouri, P., Farshi, S., Hashemi, Z., & Kasraee, B. (2015). Evaluation of the efficacy of
581 cysteamine 5% cream in the treatment of epidermal melasma: A randomized double-
582 blind placebo-controlled trial. *The British Journal of Dermatology*, 173(1), 209–217.
583 <https://doi.org/10.1111/bjd.13424>

584 Matloob, A. H., Mourtas, S., Klepetsanis, P., & Antimisiaris, S. G. (2014). Increasing the
585 stability of curcumin in serum with liposomes or hybrid drug-in-cyclodextrin-in-
586 liposome systems: A comparative study. *International Journal of Pharmaceutics*,
587 476(1–2), 108–115. <https://doi.org/10.1016/j.ijpharm.2014.09.041>

588 Okamura, D. M., Bahrami, N. M., Ren, S., Pasichnyk, K., Williams, J. M., Gangoiti, J. A.,
589 Lopez-Guisa, J. M., Yamaguchi, I., Barshop, B. A., Duffield, J. S., & Eddy, A. A.
590 (2014). Cysteamine Modulates Oxidative Stress and Blocks Myofibroblast Activity in
591 CKD. *Journal of the American Society of Nephrology : JASN*, 25(1), 43–54.
592 <https://doi.org/10.1681/ASN.2012090962>

593 Pescina, S., Carra, F., Padula, C., Santi, P., & Nicoli, S. (2016). Effect of pH and penetration
594 enhancers on cysteamine stability and trans-corneal transport. *European Journal of*
595 *Pharmaceutics and Biopharmaceutics*, *107*, 171–179.
596 <https://doi.org/10.1016/j.ejpb.2016.07.009>

597 Qiu, L., Zhang, M., Sturm, R. A., Gardiner, B., Tonks, I., Kay, G., & Parsons, P. G. (2000).
598 Inhibition of melanin synthesis by cystamine in human melanoma cells. *The Journal*
599 *of Investigative Dermatology*, *114*(1), 21–27. [https://doi.org/10.1046/j.1523-](https://doi.org/10.1046/j.1523-1747.2000.00826.x)
600 [1747.2000.00826.x](https://doi.org/10.1046/j.1523-1747.2000.00826.x)

601 Rendon, M. I., & Gaviria, J. I. (2005). Review of Skin-Lightening Agents. *Dermatologic*
602 *Surgery*, *31*(s1), 886–890. <https://doi.org/10.1111/j.1524-4725.2005.31736>

603 Rhee, S. G., Chang, T.-S., Jeong, W., & Kang, D. (2010). Methods for detection and
604 measurement of hydrogen peroxide inside and outside of cells. *Molecules and Cells*,
605 *29*(6), 539–549. <https://doi.org/10.1007/s10059-010-0082-3>

606 Ribeiro, M., Silva, A. C., Rodrigues, J., Naia, L., & Rego, A. C. (2013). Oxidizing Effects of
607 Exogenous Stressors in Huntington’s Disease Knock-in Striatal Cells—Protective
608 Effect of Cystamine and Creatine. *Toxicological Sciences*, *136*(2), 487–499.
609 <https://doi.org/10.1093/toxsci/kft199>

610 Shah, S. M., Ashtikar, M., Jain, A. S., Makhija, D. T., Nikam, Y., Gude, R. P., Steiniger, F.,
611 Jagtap, A. A., Nagarsenker, M. S., & Fahr, A. (2015). LeciPlex, invasomes, and
612 liposomes: A skin penetration study. *International Journal of Pharmaceutics*, *490*(1–
613 *2*), 391–403. <https://doi.org/10.1016/j.ijpharm.2015.05.042>

614 Shin, Y. J., Seo, J. M., Chung, T. Y., Hyon, J. Y., & Wee, W. R. (2011). Effect of Cysteamine
615 on Oxidative Stress-induced Cell Death of Human Corneal Endothelial Cells. *Current*
616 *Eye Research*, *36*(10), 910–917. <https://doi.org/10.3109/02713683.2011.593726>

617 Shiny, A., Toomu, M., & Dhurke, R. K. (2016). ENHANCED DERMAL DELIVERY OF
618 NADIFLOXACIN USING LIPOSOMES. *International Journal of Applied*
619 *Pharmaceutics*, 53–59. <https://doi.org/10.22159/ijap.2016v8i4.14315>

620 Solano, F., Briganti, S., Picardo, M., & Ghanem, G. (2006). Hypopigmenting agents: An
621 updated review on biological, chemical and clinical aspects. *Pigment Cell Research*,
622 *19(6)*, 550–571. <https://doi.org/10.1111/j.1600-0749.2006.00334.x>

623 Sun, L., Xu, S., Zhou, M., Wang, C., Wu, Y., & Chan, P. (2010). Effects of cysteamine on
624 MPTP-induced dopaminergic neurodegeneration in mice. *Brain Research*, *1335*, 74–
625 82. <https://doi.org/10.1016/j.brainres.2010.03.079>

626 Tarnowska, M., Briançon, S., Azevedo, J. R. de, Chevalier, Y., Arquier, D., Barratier, C., &
627 Bolzinger, M. (2020). The effect of vehicle on skin absorption of Mg²⁺ and Ca²⁺
628 from thermal spring water. *International Journal of Cosmetic Science*.
629 <https://doi.org/10.1111/ics.12607>

630 Verma, D. D., Verma, S., Blume, G., & Fahr, A. (2003). Liposomes increase skin penetration
631 of entrapped and non-entrapped hydrophilic substances into human skin: A skin
632 penetration and confocal laser scanning microscopy study. *European Journal of*
633 *Pharmaceutics and Biopharmaceutics*, *55(3)*, 271–277. [https://doi.org/10.1016/S0939-](https://doi.org/10.1016/S0939-6411(03)00021-3)
634 [6411\(03\)00021-3](https://doi.org/10.1016/S0939-6411(03)00021-3)

635 Wang, W., Shu, G., Lu, K., Xu, X., Sun, M., Qi, J., Huang, Q., Tan, W., & Du, Y. (2020).
636 Flexible liposomal gel dual-loaded with all-trans retinoic acid and betamethasone for
637 enhanced therapeutic efficiency of psoriasis. *Journal of Nanobiotechnology*, *18(1)*, 80.
638 <https://doi.org/10.1186/s12951-020-00635-0>

639 Wiedmann, T. S., & Naqwi, A. (2016). Pharmaceutical salts: Theory, use in solid dosage
640 forms and in situ preparation in an aerosol. *Asian Journal of Pharmaceutical Sciences*,
641 *11(6)*, 722–734. <https://doi.org/10.1016/j.ajps.2016.07.002>

642 Yan, Y., Xing, J., Xu, W., Zhao, G., Dong, K., Zhang, L., & Wang, K. (2014).
643 Hydroxypropyl- β -cyclodextrin grafted polyethyleneimine used as transdermal
644 penetration enhancer of diclofenac sodium. *International Journal of Pharmaceutics*,
645 474(1–2), 182–192. <https://doi.org/10.1016/j.ijpharm.2014.08.021>

646 Yuan, J.-J., Qin, F. G. F., Tu, J.-L., & Li, B. (2017). Preparation, Characterization, and
647 Antioxidant Activity Evaluation of Liposomes Containing Water-Soluble
648 Hydroxytyrosol from Olive. *Molecules*, 22(6), 870.
649 <https://doi.org/10.3390/molecules22060870>

650 Yücel, Ç., & Şeker Karatoprak, G. (2017). Development and evaluation of the antioxidant
651 activity of liposomes and nanospheres containing rosmarinic acid. *Farmacia*, 65.

652 Zuriarrain, A., Zuriarrain, J., Villar, M., & Berregi, I. (2015). Quantitative determination of
653 ethanol in cider by ¹H NMR spectrometry. *Food Control*, 50, 758–762.
654 <https://doi.org/10.1016/j.foodcont.2014.10.024>

655 Zylberberg, C., & Matosevic, S. (2016). Pharmaceutical liposomal drug delivery: A review of
656 new delivery systems and a look at the regulatory landscape. *Drug Delivery*, 23(9),
657 3319–3329. <https://doi.org/10.1080/10717544.2016.1177136>

658

659

660

661 **Figure legends**

662 **Figure 1:** The structure of the different forms of cyst.

663 **Figure 2:** Stability study at 4°C of free cyst HCl, suspended cyst HCl-loaded liposome, and
664 freeze dried form of cyst HCl-loaded liposome suspended in water the day of HPLC analysis.

665 **Figure 3:** Cell viability of B16 melanoma cells in presence of different concentrations of cyst
666 HCl and cystamine (A) and in presence of free, total and encapsulated cyst HCl-loaded
667 liposome in suspension and resuspended freeze-dried form (B). Data are presented as means ±
668 SD (n = 6).

669 **Figure 4:** Inhibition percentages of melanin (A) and tyrosinase (B) for cyst HCl, cystamine,
670 kojic acid, total and encapsulated cyst HCl-loaded liposome in suspension and resuspended
671 freeze-dried forms after 2 treatments in 72 h incubation time. Data are presented as means ±
672 SD (n = 6). Statistical analysis was performed using ANOVA test; ns: not significant, *p < 0.05,
673 **p < 0.01, ***p < 0.001, ****p < 0.0001.

674 **Figure 5:** Microscopic observations of cells after 72 h of incubation with the different
675 formulations (2 treatments) and representative image of the different solubilized pellets
676 obtained ((1)Total cyst HCl loaded liposome (2) Encapsulated cyst HCl loaded liposome (3)
677 Resuspended freeze-dried cyst HCl loaded liposome (4) Cyst HCl (5) Cystamine (6) Kojic acid)

678 **Figure 6:** Intracellular ROS formation measured by relative DCFH-DA fluorescence in
679 cultured B16 pretreated by H₂O₂ and treated with 60 μM of cyst HCl and cystamine; total and
680 encapsulated cyst HCl-loaded liposome in suspension and resuspended freeze-dried forms. The
681 formation of ROS was assayed by measuring the fluorescence of DCFH-DA. Data are presented
682 as means ± SD (n = 6). Statistical analysis was performed using ANOVA test; ***p < 0.001,
683 ****p < 0.0001.

684 **Figure 7:** Fluorescence microscopy images of B16 cells pretreated with H₂O₂ and treated for
685 72 h with free and encapsulated cyst HCl and cystamine.

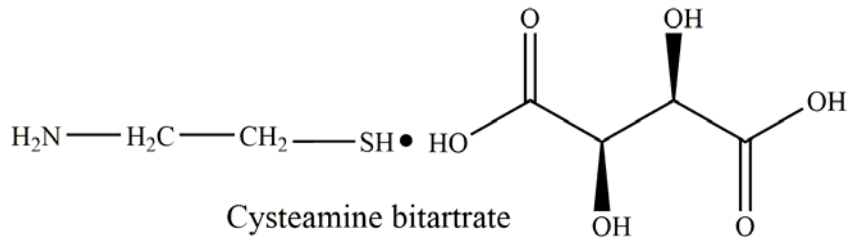
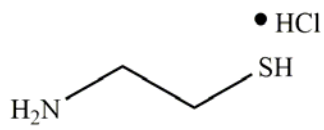
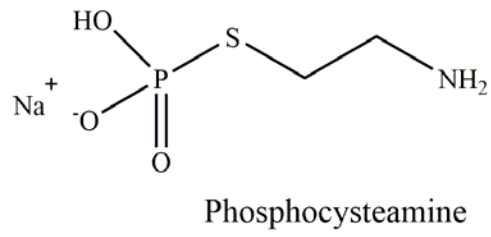
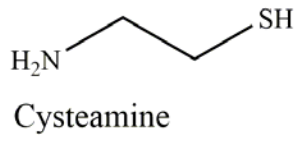
686 **Figure 8:** Skin permeation profile of free and cyst HCl loaded liposome in suspension and
687 resuspended freeze-dried forms.

688 **Figure 9:** Cyst HCl retention in the epidermis for the free, total and encapsulated cyst HCl-
689 loaded liposome in suspension and resuspended freeze-dried forms.

690

691 Figure 1

692



693

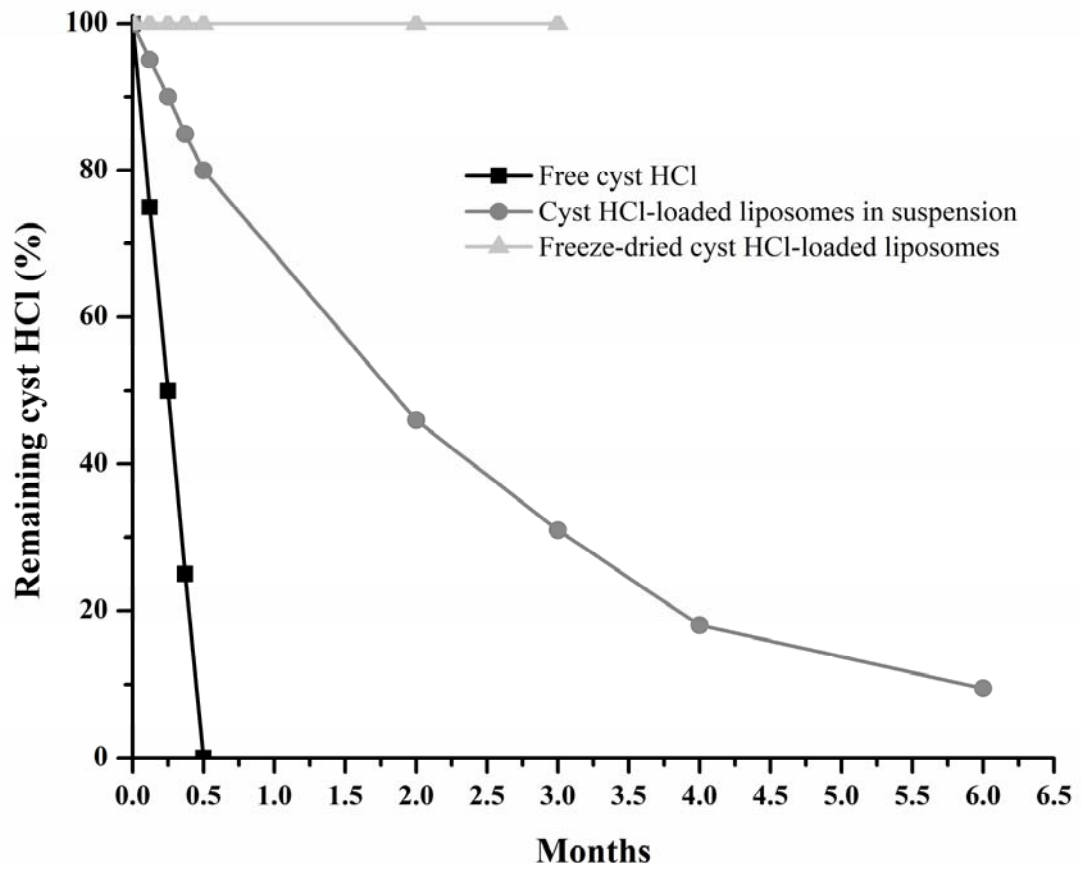
694

695

696

697 Figure 2

698



699

700

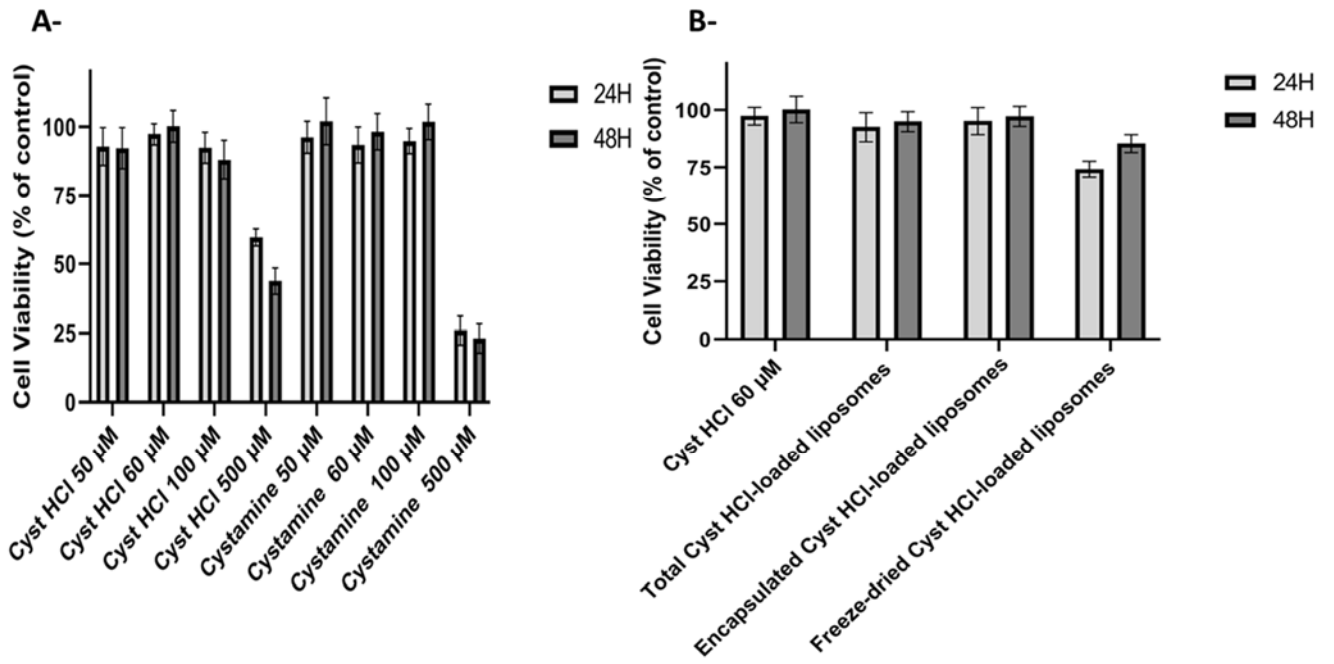
701

702

703 Figure 3

704

705



706

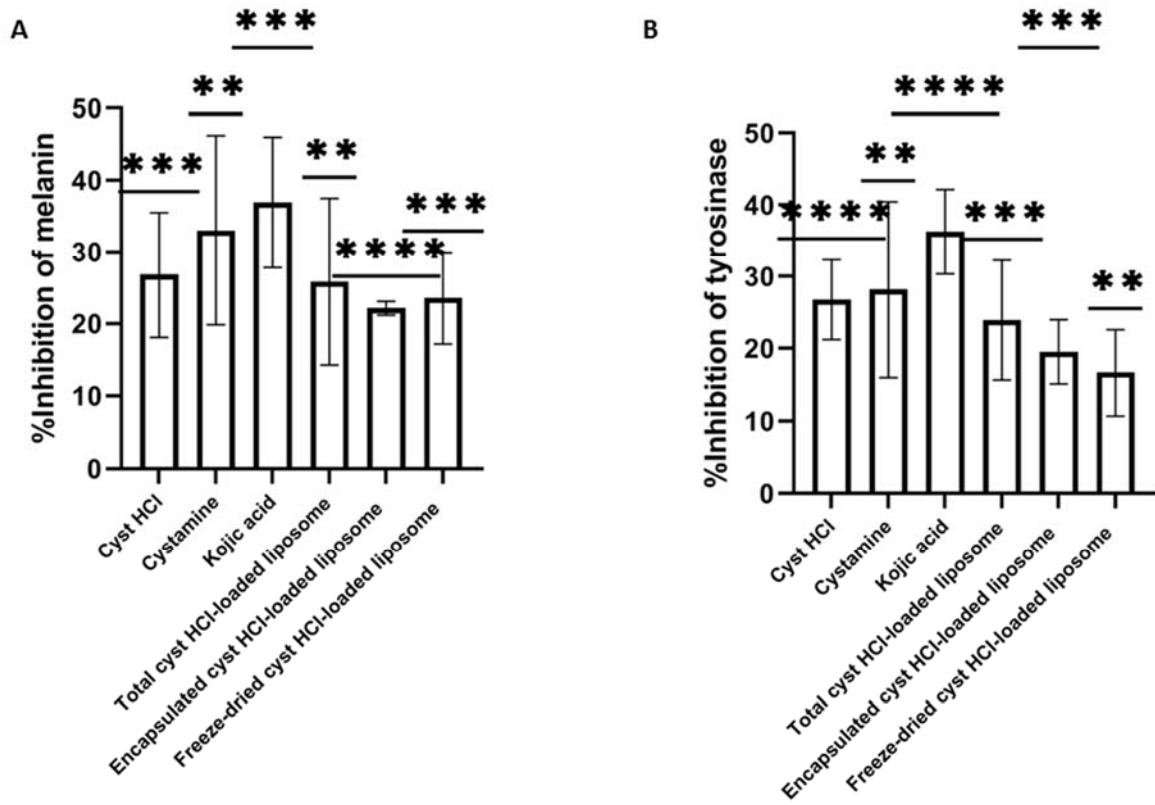
707

708

709 Figure 4

710

711



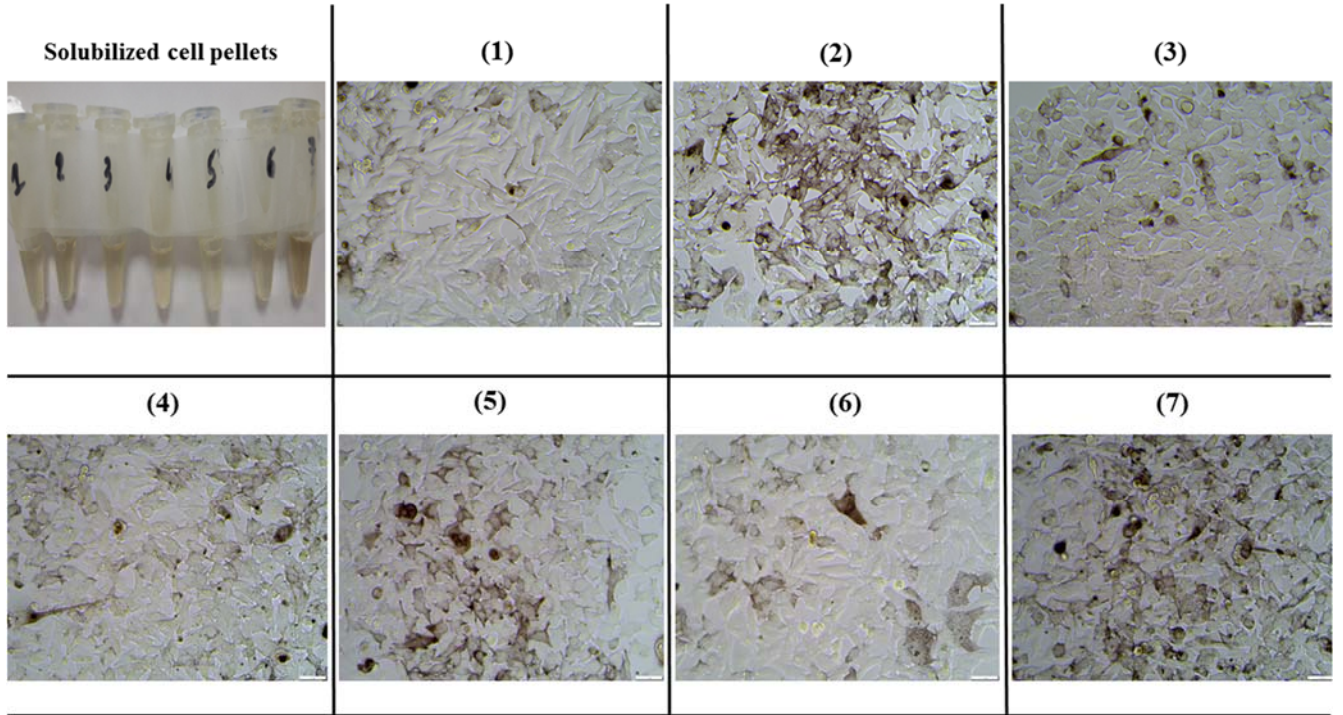
712

713

714 Figure 5

715

716



717

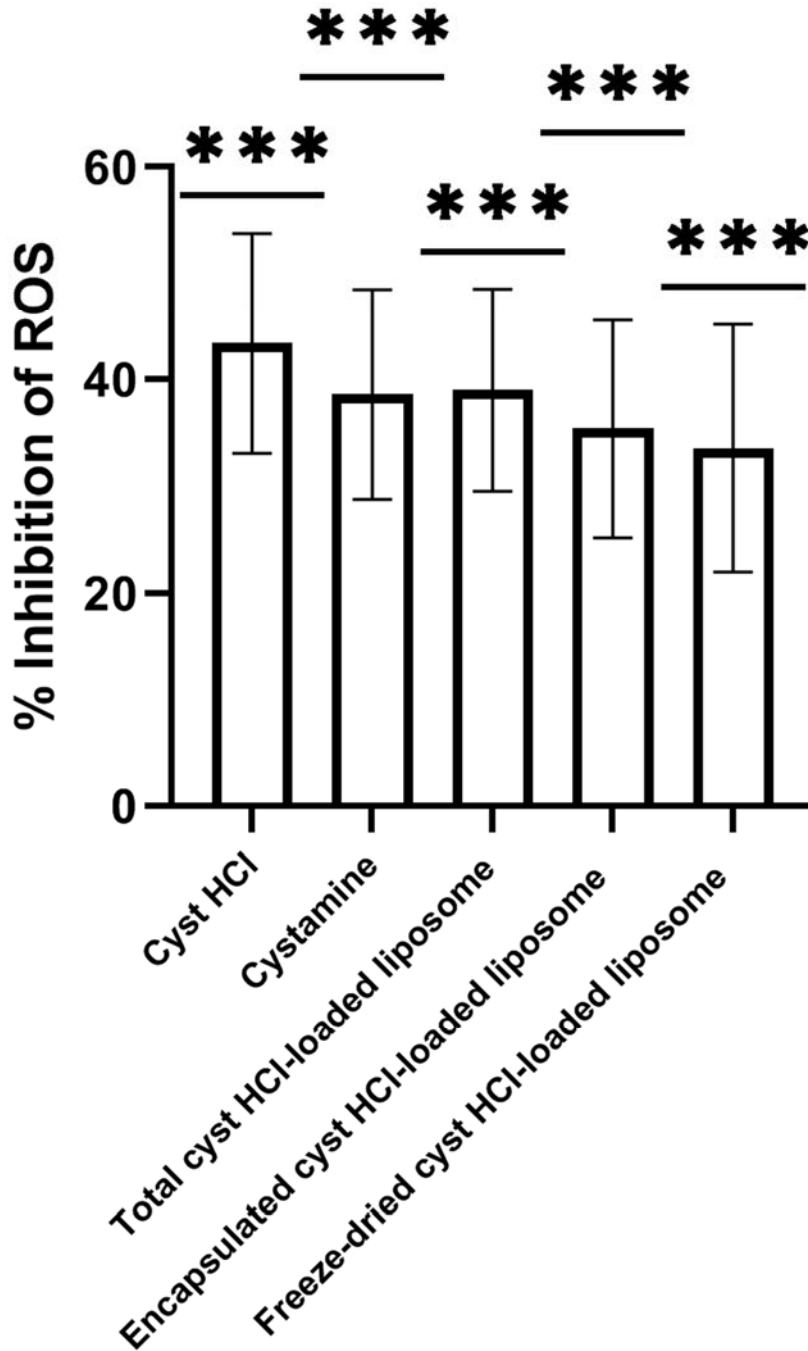
718

719

720

721 Figure 6

722



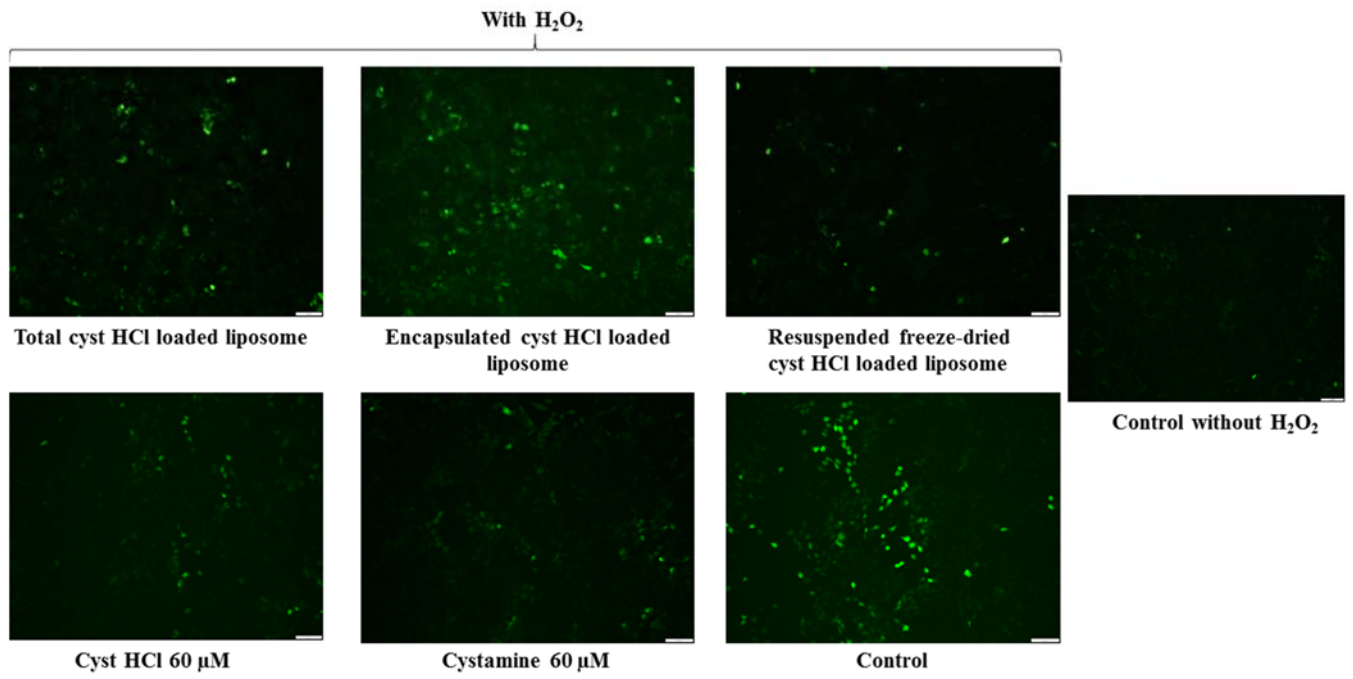
723

724

725

726 Figure 7

727



728

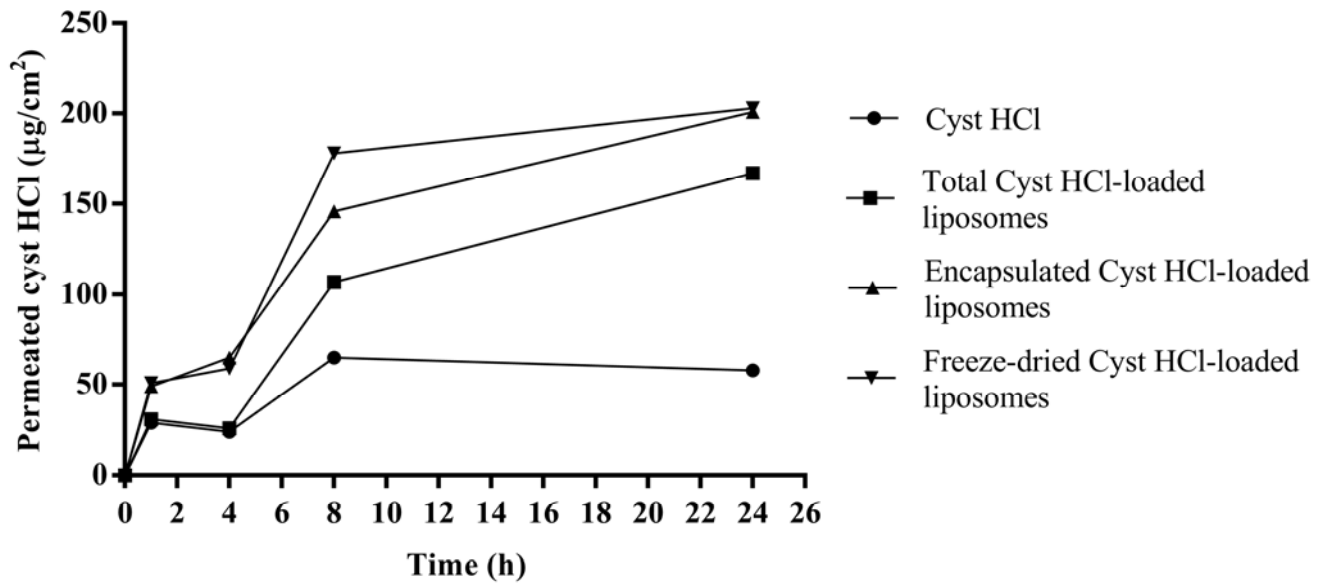
729

730

731 Figure 8

732

733



734

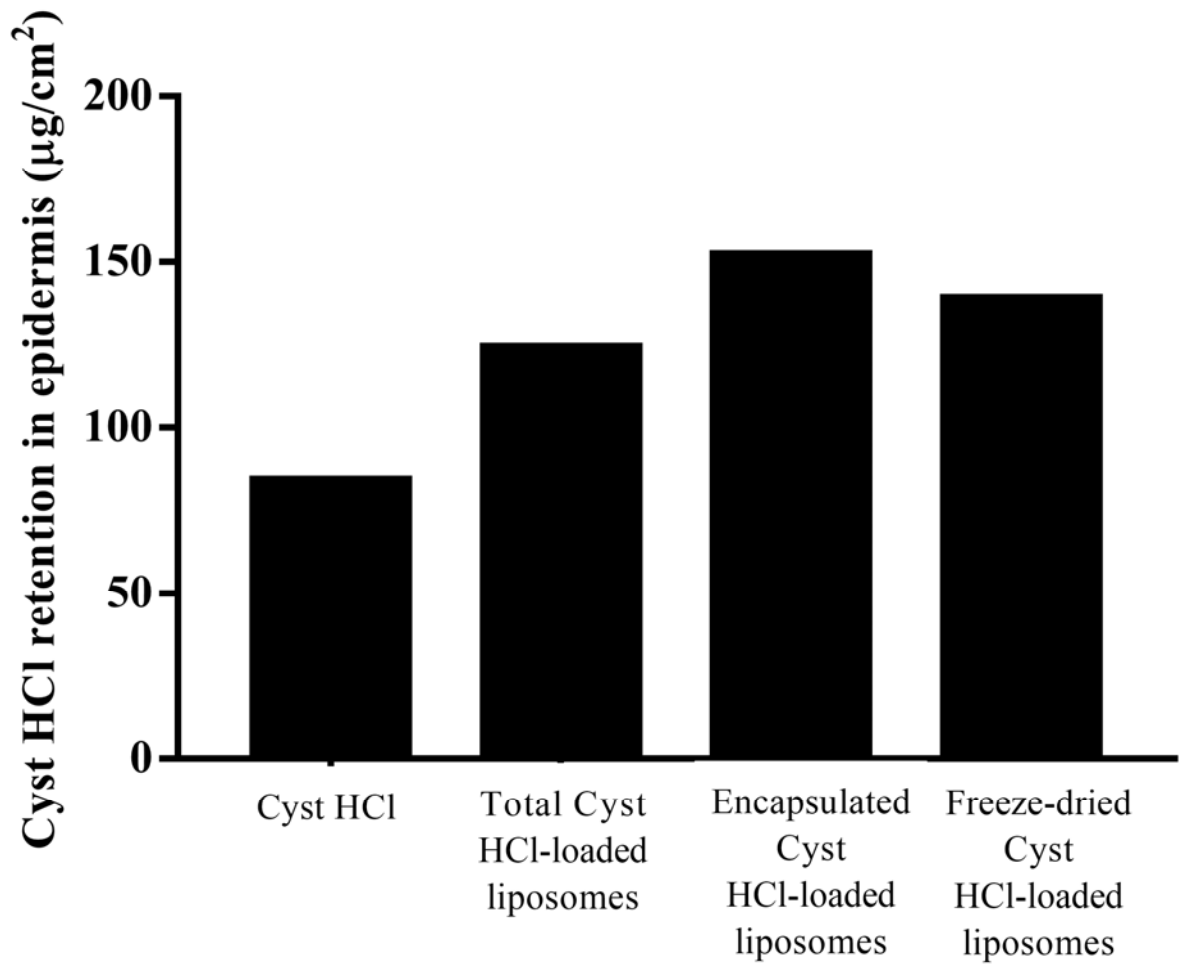
735

736

737 Figure 9

738

739



740

741

742